

The gluon spin contribution to the proton spin from the double helicity asymmetry in inclusive π^0 production in polarized $p + p$ collisions at $\sqrt{s} = 200$ GeV

A. Adare,¹² S. Afanasiev,²⁶ C. Aidala,³⁷ N.N. Ajitanand,⁵⁴ Y. Akiba,^{48,49} H. Al-Bataineh,⁴³ J. Alexander,⁵⁴ K. Aoki,^{31,48} L. Aphecetche,⁵⁶ J. Asai,⁴⁸ E.T. Atomssa,³² R. Averbeck,⁵⁵ T.C. Awes,⁴⁴ B. Azmoun,⁷ V. Babintsev,²² M. Bai,⁶ G. Baksay,¹⁸ L. Baksay,¹⁸ A. Baldissieri,¹⁵ K.N. Barish,⁸ P.D. Barnes,³⁴ B. Bassalleck,⁴² A.T. Basye,¹ S. Bathe,⁸ S. Batsouli,⁴⁴ V. Baublis,⁴⁷ C. Baumann,³⁸ A. Bazilevsky,⁷ S. Belikov,^{7,*} R. Bennett,⁵⁵ A. Berdnikov,⁵¹ Y. Berdnikov,⁵¹ A.A. Bickley,¹² J.G. Boissevain,³⁴ H. Borel,¹⁵ K. Boyle,⁵⁵ M.L. Brooks,³⁴ H. Buesching,⁷ V. Bumazhnov,²² G. Bunce,^{7,49} S. Butsyk,³⁴ C.M. Camacho,³⁴ S. Campbell,⁵⁵ P. Chand,⁴ B.S. Chang,⁶³ W.C. Chang,² J.-L. Charvet,¹⁵ S. Chernichenko,²² C.Y. Chi,¹³ M. Chiu,²³ I.J. Choi,⁶³ R.K. Choudhury,⁴ T. Chujo,⁵⁹ P. Chung,⁵⁴ A. Churyn,²² V. Cianciolo,⁴⁴ B.A. Cole,¹³ P. Constantin,³⁴ M. Csanád,¹⁷ T. Csörgő,²⁸ T. Dahms,⁵⁵ S. Dairaku,^{31,48} K. Das,¹⁹ G. David,⁷ A. Denisov,²² D. d'Enterria,³² A. Deshpande,^{49,55} E.J. Desmond,⁷ O. Dietzsch,⁵² A. Dion,⁵⁵ M. Donadelli,⁵² O. Drapier,³² A. Drees,⁵⁵ K.A. Drees,⁶ A.K. Dubey,⁶² A. Durum,²² D. Dutta,⁴ V. Dzhordzhadze,⁸ Y.V. Efremenko,⁴⁴ J. Egdemir,⁵⁵ F. Ellinghaus,¹² T. Engelmores,¹³ A. Enokizono,³³ H. En'yo,^{48,49} S. Esumi,⁵⁹ K.O. Eyser,⁸ B. Fadem,³⁹ D.E. Fields,^{42,49} M. Finger,⁹ M. Finger, Jr.,⁹ F. Fleuret,³² S.L. Fokin,³⁰ Z. Fraenkel,^{62,*} J.E. Frantz,⁵⁵ A. Franz,⁷ A.D. Frawley,¹⁹ K. Fujiwara,⁴⁸ Y. Fukao,^{31,48} T. Fusayasu,⁴¹ I. Garishvili,⁵⁷ A. Glenn,¹² H. Gong,⁵⁵ M. Gonin,³² J. Gosset,¹⁵ Y. Goto,^{48,49} R. Granier de Cassagnac,³² N. Grau,¹³ S.V. Greene,⁶⁰ M. Grosse Perdekamp,^{23,49} T. Gunji,¹¹ H.-Å. Gustafsson,³⁶ A. Hadj Henni,⁵⁶ J.S. Haggerty,⁷ H. Hamagaki,¹¹ R. Han,⁴⁶ E.P. Hartouni,³³ K. Haruna,²¹ E. Haslum,³⁶ R. Hayano,¹¹ M. Heffner,³³ T.K. Hemmick,⁵⁵ T. Hester,⁸ X. He,²⁰ J.C. Hill,²⁵ M. Hohlmann,¹⁸ W. Holzmann,⁵⁴ K. Homma,²¹ B. Hong,²⁹ T. Horaguchi,^{11,48,58} D. Hornback,⁵⁷ S. Huang,⁶⁰ T. Ichihara,^{48,49} R. Ichimiya,⁴⁸ Y. Ikeda,⁵⁹ K. Imai,^{31,48} J. Imrek,¹⁶ M. Inaba,⁵⁹ D. Isenhower,¹ M. Ishihara,⁴⁸ T. Isobe,¹¹ M. Issah,⁵⁴ A. Isupov,²⁶ D. Ivanishev,⁴⁷ B.V. Jacak,^{55,†} J. Jia,¹³ J. Jin,¹³ B.M. Johnson,⁷ K.S. Joo,⁴⁰ D. Jouan,⁴⁵ F. Kajihara,¹¹ S. Kametani,⁴⁸ N. Kamihara,⁴⁹ J. Kamin,⁵⁵ J.H. Kang,⁶³ J. Kapustinsky,³⁴ D. Kawall,^{37,49} A.V. Kazantsev,³⁰ T. Kempel,²⁵ A. Khanzadeev,⁴⁷ K. Kijima,²¹ J. Kikuchi,⁶¹ B.I. Kim,²⁹ D.H. Kim,⁴⁰ D.J. Kim,⁶³ E. Kim,⁵³ S.H. Kim,⁶³ E. Kinney,¹² K. Kiriluk,¹² A. Kiss,¹⁷ E. Kistenev,⁷ J. Klay,³³ C. Klein-Boesing,³⁸ L. Kochenda,⁴⁷ V. Kochetkov,²² B. Komkov,⁴⁷ M. Konno,⁵⁹ J. Koster,²³ A. Kozlov,⁶² A. Král,¹⁴ A. Kravitz,¹³ G.J. Kunde,³⁴ K. Kurita,^{50,48} M. Kurosawa,⁴⁸ M.J. Kweon,²⁹ Y. Kwon,⁵⁷ G.S. Kyle,⁴³ R. Lacey,⁵⁴ Y.S. Lai,¹³ J.G. Lajoie,²⁵ D. Layton,²³ A. Lebedev,²⁵ D.M. Lee,³⁴ K.B. Lee,²⁹ T. Lee,⁵³ M.J. Leitch,³⁴ M.A.L. Leite,⁵² B. Lenzi,⁵² P. Liebing,⁴⁹ T. Liška,¹⁴ A. Litvinenko,²⁶ H. Liu,⁴³ M.X. Liu,³⁴ X. Li,¹⁰ B. Love,⁶⁰ D. Lynch,⁷ C.F. Maguire,⁶⁰ Y.I. Makdisi,⁶ A. Malakhov,²⁶ M.D. Malik,⁴² V.I. Manko,³⁰ E. Mannel,¹³ Y. Mao,^{46,48} L. Mašek,^{9,24} H. Masui,⁵⁹ F. Matathias,¹³ M. McCumber,⁵⁵ P.L. McGaughey,³⁴ B. Meredith,²³ Y. Miake,⁵⁹ P. Mikeš,²⁴ K. Miki,⁵⁹ A. Milov,⁷ M. Mishra,³ J.T. Mitchell,⁷ A.K. Mohanty,⁴ Y. Morino,¹¹ A. Morreale,⁸ D.P. Morrison,⁷ T.V. Moukhanova,³⁰ D. Mukhopadhyay,⁶⁰ J. Murata,^{50,48} S. Nagamiya,²⁷ J.L. Nagle,¹² M. Naglis,⁶² M. Nagy,¹⁷ I. Nakagawa,^{48,49} Y. Nakamiya,²¹ T. Nakamura,²¹ K. Nakano,^{48,58} J. Newby,³³ M. Nguyen,⁵⁵ T. Niita,⁵⁹ R. Nouicer,⁵ A.S. Nyanin,³⁰ E. O'Brien,⁷ S.X. Oda,¹¹ C.A. Ogilvie,²⁵ H. Okada,^{31,48} K. Okada,⁴⁹ M. Oka,⁵⁹ Y. Onuki,⁴⁸ A. Oskarsson,³⁶ M. Ouchida,²¹ K. Ozawa,¹¹ R. Pak,⁵ A.P.T. Palounek,³⁴ V. Pantuev,⁵⁵ V. Papavassiliou,⁴³ J. Park,⁵³ W.J. Park,²⁹ S.F. Pate,⁴³ H. Pei,²⁵ J.-C. Peng,²³ H. Pereira,¹⁵ V. Peresedov,²⁶ D.Yu. Peressounko,³⁰ C. Pinkenburg,⁷ M.L. Porschke,⁷ A.K. Purwar,³⁴ H. Qu,²⁰ J. Rak,⁴² A. Rakotozafindrabe,³² I. Ravinovich,⁶² K.F. Read,^{44,57} S. Rembeczki,¹⁸ M. Reuter,⁵⁵ K. Reygers,³⁸ V. Riabov,⁴⁷ Y. Riabov,⁴⁷ D. Roach,⁶⁰ G. Roche,³⁵ S.D. Rolnick,⁸ M. Rosati,²⁵ S.S.E. Rosendahl,³⁶ P. Rosnet,³⁵ P. Rukoyatkin,²⁶ P. Ružička,²⁴ V.L. Rykov,⁴⁸ B. Sahlmueller,³⁸ N. Saito,^{31,48,49} T. Sakaguchi,⁷ S. Sakai,⁵⁹ K. Sakashita,^{48,58} V. Samsonov,⁴⁷ T. Sato,⁵⁹ S. Sawada,²⁷ K. Sedgwick,⁸ J. Seele,¹² R. Seidl,²³ A.Yu. Semenov,²⁵ V. Semenov,²² R. Seto,⁸ D. Sharma,⁶² I. Shein,²² T.-A. Shibata,^{48,58} K. Shigaki,²¹ M. Shimomura,⁵⁹ K. Shoji,^{31,48} P. Shukla,⁴ A. Sickles,⁷ C.L. Silva,⁵² D. Silvermyr,⁴⁴ C. Silvestre,¹⁵ K.S. Sim,²⁹ B.K. Singh,³ C.P. Singh,³ V. Singh,³ M. Slunečka,⁹ A. Soldatov,²² R.A. Soltz,³³ W.E. Sondheim,³⁴ S.P. Sorensen,⁵⁷ I.V. Sourikova,⁷ F. Staley,¹⁵ P.W. Stankus,⁴⁴ E. Stenlund,³⁶ M. Stepanov,⁴³ A. Ster,²⁸ S.P. Stoll,⁷ T. Sugitate,²¹ C. Suire,⁴⁵ A. Sukhanov,⁵ J. Sziklai,²⁸ E.M. Takagui,⁵² A. Taketani,^{48,49} R. Tanabe,⁵⁹ Y. Tanaka,⁴¹ S. Taneja,⁵⁵ K. Tanida,^{48,49} M.J. Tannenbaum,⁷ A. Taranenko,⁵⁴ P. Tarján,¹⁶ T.L. Thomas,⁴² M. Togawa,^{31,48} A. Toia,⁵⁵ L. Tomášek,²⁴ Y. Tomita,⁵⁹ H. Torii,⁴⁸ R.S. Towell,¹ V.-N. Tram,³² I. Tserruya,⁶² Y. Tsuchimoto,²¹ C. Vale,²⁵ H. Valle,⁶⁰ H.W. van Hecke,³⁴ A. Veicht,²³ J. Velkovska,⁶⁰ R. Vertesi,¹⁶ A.A. Vinogradov,³⁰ M. Virius,¹⁴ V. Vrba,²⁴ E. Vznuzdaev,⁴⁷ D. Walker,⁵⁵ X.R. Wang,⁴³ Y. Watanabe,^{48,49}

F. Wei,²⁵ J. Wessels,³⁸ S.N. White,⁷ S. Williamson,²³ D. Winter,¹³ C.L. Woody,⁷ M. Wysocki,¹² W. Xie,⁴⁹
 Y.L. Yamaguchi,⁶¹ K. Yamaura,²¹ R. Yang,²³ A. Yanovich,²² J. Ying,²⁰ S. Yokkaichi,^{48,49} G.R. Young,⁴⁴
 I. Younus,⁴² I.E. Yushmanov,³⁰ W.A. Zajc,¹³ O. Zaudtke,³⁸ C. Zhang,⁴⁴ S. Zhou,¹⁰ and L. Zolin²⁶

(PHENIX Collaboration)

- ¹Abilene Christian University, Abilene, TX 79699, U.S.
²Institute of Physics, Academia Sinica, Taipei 11529, Taiwan
³Department of Physics, Banaras Hindu University, Varanasi 221005, India
⁴Bhabha Atomic Research Centre, Bombay 400 085, India
⁵Chemistry Department, Brookhaven National Laboratory, Upton, NY 11973-5000, U.S.
⁶Collider-Accelerator Department, Brookhaven National Laboratory, Upton, NY 11973-5000, U.S.
⁷Physics Department, Brookhaven National Laboratory, Upton, NY 11973-5000, U.S.
⁸University of California - Riverside, Riverside, CA 92521, U.S.
⁹Charles University, Ovocný trh 5, Praha 1, 116 36, Prague, Czech Republic
¹⁰China Institute of Atomic Energy (CIAE), Beijing, People's Republic of China
¹¹Center for Nuclear Study, Graduate School of Science, University of Tokyo, 7-3-1 Hongo, Bunkyo, Tokyo 113-0033, Japan
¹²University of Colorado, Boulder, CO 80309, U.S.
¹³Columbia University, New York, NY 10027 and Nevis Laboratories, Irvington, NY 10533, U.S.
¹⁴Czech Technical University, Zikova 4, 166 36 Prague 6, Czech Republic
¹⁵Dapnia, CEA Saclay, F-91191, Gif-sur-Yvette, France
¹⁶Debrecen University, H-4010 Debrecen, Egyetem tér 1, Hungary
¹⁷ELTE, Eötvös Loránd University, H - 1117 Budapest, Pázmány P. s. 1/A, Hungary
¹⁸Florida Institute of Technology, Melbourne, FL 32901, U.S.
¹⁹Florida State University, Tallahassee, FL 32306, U.S.
²⁰Georgia State University, Atlanta, GA 30303, U.S.
²¹Hiroshima University, Kagamiyama, Higashi-Hiroshima 739-8526, Japan
²²IHEP Protvino, State Research Center of Russian Federation, Institute for High Energy Physics, Protvino, 142281, Russia
²³University of Illinois at Urbana-Champaign, Urbana, IL 61801, U.S.
²⁴Institute of Physics, Academy of Sciences of the Czech Republic, Na Slovance 2, 182 21 Prague 8, Czech Republic
²⁵Iowa State University, Ames, IA 50011, U.S.
²⁶Joint Institute for Nuclear Research, 141980 Dubna, Moscow Region, Russia
²⁷KEK, High Energy Accelerator Research Organization, Tsukuba, Ibaraki 305-0801, Japan
²⁸KFKI Research Institute for Particle and Nuclear Physics of the Hungarian Academy of Sciences (MTA KFKI RMKI), H-1525 Budapest 114, POBox 49, Budapest, Hungary
²⁹Korea University, Seoul, 136-701, Korea
³⁰Russian Research Center "Kurchatov Institute", Moscow, Russia
³¹Kyoto University, Kyoto 606-8502, Japan
³²Laboratoire Leprince-Ringuet, Ecole Polytechnique, CNRS-IN2P3, Route de Saclay, F-91128, Palaiseau, France
³³Lawrence Livermore National Laboratory, Livermore, CA 94550, U.S.
³⁴Los Alamos National Laboratory, Los Alamos, NM 87545, U.S.
³⁵LPC, Université Blaise Pascal, CNRS-IN2P3, Clermont-Fd, 63177 Aubiere Cedex, France
³⁶Department of Physics, Lund University, Box 118, SE-221 00 Lund, Sweden
³⁷Department of Physics, University of Massachusetts, Amherst, MA 01003-9337, U.S.
³⁸Institut für Kernphysik, University of Muenster, D-48149 Muenster, Germany
³⁹Muhlenberg University, Allentown, PA 18104-5586, U.S.
⁴⁰Myongji University, Yongin, Kyonggido 449-728, Korea
⁴¹Nagasaki Institute of Applied Science, Nagasaki-shi, Nagasaki 851-0193, Japan
⁴²University of New Mexico, Albuquerque, NM 87131, U.S.
⁴³New Mexico State University, Las Cruces, NM 88003, U.S.
⁴⁴Oak Ridge National Laboratory, Oak Ridge, TN 37831, U.S.
⁴⁵IPN-Orsay, Université Paris Sud, CNRS-IN2P3, BP1, F-91406, Orsay, France
⁴⁶Peking University, Beijing, People's Republic of China
⁴⁷PNPI, Petersburg Nuclear Physics Institute, Gatchina, Leningrad region, 188300, Russia
⁴⁸RIKEN, The Institute of Physical and Chemical Research, Wako, Saitama 351-0198, Japan
⁴⁹RIKEN BNL Research Center, Brookhaven National Laboratory, Upton, NY 11973-5000, U.S.
⁵⁰Physics Department, Rikkyo University, 3-34-1 Nishi-Ikebukuro, Toshima, Tokyo 171-8501, Japan
⁵¹Saint Petersburg State Polytechnic University, St. Petersburg, Russia
⁵²Universidade de São Paulo, Instituto de Física, Caixa Postal 66318, São Paulo CEP05315-970, Brazil
⁵³System Electronics Laboratory, Seoul National University, Seoul, Korea
⁵⁴Chemistry Department, Stony Brook University, Stony Brook, SUNY, NY 11794-3400, U.S.
⁵⁵Department of Physics and Astronomy, Stony Brook University, SUNY, Stony Brook, NY 11794, U.S.
⁵⁶SUBATECH (Ecole des Mines de Nantes, CNRS-IN2P3, Université de Nantes) BP 20722 - 44307, Nantes, France
⁵⁷University of Tennessee, Knoxville, TN 37996, U.S.

⁵⁸Department of Physics, Tokyo Institute of Technology, Oh-okayama, Meguro, Tokyo 152-8551, Japan

⁵⁹Institute of Physics, University of Tsukuba, Tsukuba, Ibaraki 305, Japan

⁶⁰Vanderbilt University, Nashville, TN 37235, U.S.

⁶¹Waseda University, Advanced Research Institute for Science and Engineering, 17 Kikui-cho, Shinjuku-ku, Tokyo 162-0044, Japan

⁶²Weizmann Institute, Rehovot 76100, Israel

⁶³Yonsei University, IPAP, Seoul 120-749, Korea

(Dated: October 25, 2018)

The double helicity asymmetry in neutral pion production for $p_T = 1$ to 12 GeV/c has been measured with the PHENIX experiment in order to access the gluon spin contribution, ΔG , to the proton spin. Measured asymmetries are consistent with zero, and at a theory scale of $\mu^2 = 4$ GeV² give $\Delta G^{[0.02,0.3]} = 0.1$ to 0.2, with a constraint of $-0.7 < \Delta G^{[0.02,0.3]} < 0.5$ at $\Delta\chi^2 = 9$ ($\sim 3\sigma$) for our sampled gluon momentum fraction (x) range, 0.02 to 0.3. The results are obtained using predictions for our measured asymmetries generated from four representative fits to polarized deep inelastic scattering data. We also consider the dependence of the ΔG constraint on the choice of theoretical scale, a dominant uncertainty in these predictions.

PACS numbers: 13.85.Ni,13.88.+e,21.10.Hw,25.40.Ep

The quark spin contribution to the proton spin was found to be only $\sim 25\%$ [1, 2, 3], indicating that the majority of the proton spin on average comes from the gluon spin contribution, ΔG , and/or from gluon and quark orbital angular momentum. High energy polarized proton-proton collisions at the Relativistic Heavy Ion Collider (RHIC) at Brookhaven National Laboratory access ΔG at leading order through spin-dependent gluon-gluon (gg) and quark-gluon (qg) scattering.

This paper presents results from the 2006 RHIC run (Run-6) on ΔG from measurements of the double helicity asymmetry (A_{LL}) in inclusive mid-rapidity π^0 production by the PHENIX experiment. ΔG can be extracted from $A_{LL}^{\pi^0}$ using next to leading order (NLO) perturbative quantum chromodynamics (pQCD) [4], which successfully describes unpolarized cross-sections measured at RHIC for many inclusive processes [5, 6, 7], including mid-rapidity π^0 production [8], at $\sqrt{s}=200$ GeV. These data represent a factor of two improvement in the statistical uncertainty compared to previous results [8, 9, 10]. They significantly constrain ΔG , as presented in a recent global fit (DSSV) [11] of both RHIC and polarized deep inelastic scattering (pDIS) data, which used a preliminary version of these results. We further present the impact of experimental systematic and several theoretical uncertainties on our determination of ΔG .

We define $\Delta G^{[a,b]} \equiv \int_a^b dx \Delta g(x, \mu^2)$, with $\Delta g(x, \mu^2)$, the polarized gluon distribution, a function of x , the gluon momentum fraction and μ^2 , the factorization scale. Thus $\Delta G^{[0,1]} \equiv \Delta G$. Figure 1a shows the best fit $\Delta g(x)$ from four different pDIS fits: GRSV-std [12], BB (“ISET-4”) [13], LSS [14] and GS-C [15] which assumes a node, or sign change, in $\Delta g(x)$. As the pDIS data have limited sensitivity to ΔG , there remains large uncertainty, which was estimated by BB, and is shown as the hatched band. The result from the recent global fit, DSSV, is also shown. It has a node, which is driven by the inclusion of RHIC PHENIX π^0 and STAR jet [16, 17] A_{LL} data

along with evolution from pDIS at large x [11]. Table I lists $\Delta G^{[a,b]}$ for several x ranges.

We define $A_{LL}^{\pi^0} = (\sigma_{++} - \sigma_{+-}) / (\sigma_{++} + \sigma_{+-})$, with σ_{++} (σ_{+-}) the beam helicity dependent differential cross sections for inclusive π^0 production from collisions of longitudinally polarized protons with the same (opposite) helicity. The asymmetry is measured using

$$A_{LL}^{\pi^0} = \frac{1}{\langle P_B P_Y \rangle} \frac{N_{++} - RN_{+-}}{N_{++} + RN_{+-}}, \quad R = \frac{L_{++}}{L_{+-}} \quad (1)$$

where P_B and P_Y are the polarizations of the two RHIC beams, called “Blue” and “Yellow,” and R , the relative luminosity, is the ratio of integrated luminosities (L) for same and opposite helicity collisions. Here we take N to be the π^0 yield in a transverse momentum (p_T) bin.

Each π^0 p_T bin samples a distribution in gluon x . Figure 1b shows the sampled gluon x distributions for three

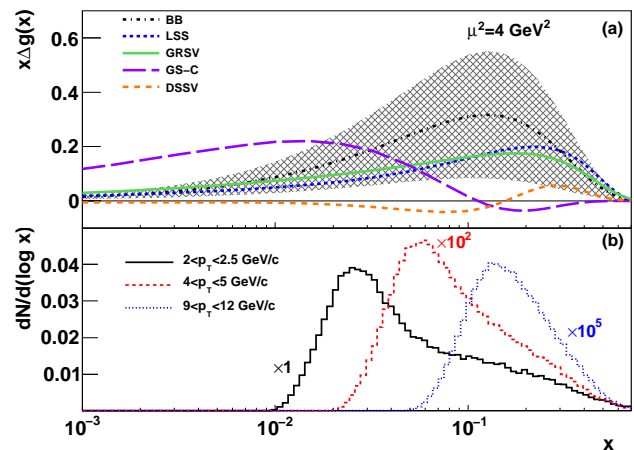


FIG. 1: (color online) (a) The polarized gluon distribution as a function of x for five fits to polarized data. Hatched band is pDIS 1σ uncertainty (BB). (b) Distributions of gluon x in three π^0 p_T bins from a NLO pQCD simulation.

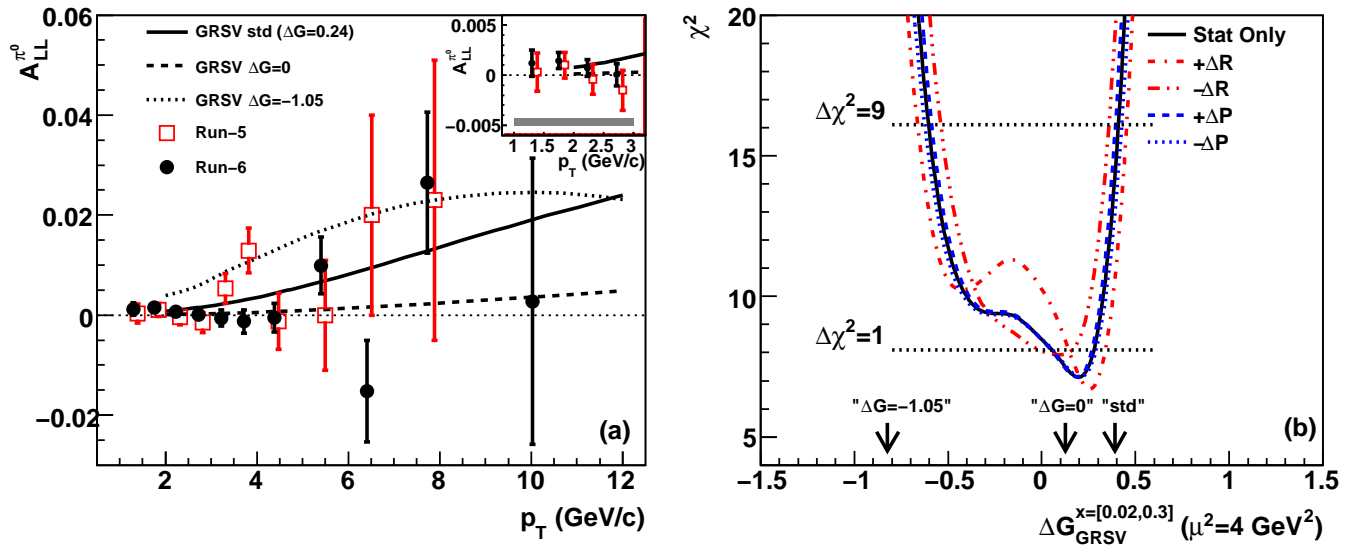


FIG. 2: (color online) (a) Asymmetry in π^0 production as a function of p_T . Error bars are statistical uncertainties. An 8.3% scale uncertainty due to the uncertainty in beam polarization is not shown. The p_T independent uncertainty of 7×10^{-4} due to relative luminosity is shown only in the inset as a shaded bar. For comparison, we also show our Run-5 result. NLO pQCD expectations based on different inputs for ΔG in the GRSV parameterization are plotted. (b) The χ^2 profile as a function of $\Delta G_{\text{GRSV}}^{x=[0.02,0.3]}$ using the combined Run5 and Run6 data considering only statistical uncertainty, or also varying by $\pm 1\sigma$ the two primary experimental systematic uncertainties, from beam polarizations ($\pm \Delta P$) and relative luminosity ($\pm \Delta R$).

$A_{\text{LL}}^{\pi^0}$ p_T bins from a NLO pQCD simulation [4, 18]. They are peaked at $x_T/0.7$ [19], with $x_T \equiv p_T/(\sqrt{s}/2)$. The bins overlap, with our data covering primarily the range $0.02 < x < 0.3$, and so we probe $\Delta G^{[0.02,0.3]}$.

The highly segmented PHENIX electromagnetic calorimeter (EMCal) [20] is used to detect $\pi^0 \rightarrow \gamma\gamma$ decays. The EMCal covers a pseudorapidity range of $|\eta| < 0.35$ and azimuthal angle range of $\Delta\phi = \pi$, with segmentation $\Delta\eta \times \Delta\phi = 0.01 \times 0.01$. We required for each of the two decay photons an energy deposition pattern consistent with an electromagnetic shower, no charged track pointing to the location of the deposited energy, and standard quality assurance requirements [9]. Events were obtained from an EMCal based high p_T photon trigger [21] in coincidence with a minimum bias trigger [8] (also used to obtain the relative luminosity). This EMCal based trigger had an efficiency for π^0 of 5% at $p_T \approx 1$ GeV/c and 90% for $p_T > 3.5$ GeV/c. The minimum bias trigger was defined as the coincidence of signals from forward and backward beam-beam counters (BBC) with full azimuthal coverage located at pseudorapidities $\pm(3.0-3.9)$ [22]. The analyzed data sample corresponded to an integrated luminosity of 6.5 pb^{-1} .

Each collider ring of RHIC was filled with up to 111 out of a possible 120 bunches, spaced 106 ns apart, with bunch helicities set such that all four beam helicity combinations occurred in sequences of four bunch crossings. The pattern of helicity combinations for each RHIC fill (typically 8 hrs) was cycled between four possibilities in order to reduce systematic uncertainties that

could be correlated to the bunch structure in RHIC [8]. Events were tagged with the bunch crossing number to obtain the beam helicities for the event. The luminosity weighted beam polarization product was $\langle P_B P_Y \rangle = 0.322 \pm 0.027$ (8.3%), with single beam polarizations of 0.560 and 0.575. Using very forward neutron production asymmetry [8, 23], the longitudinal polarization fractions were found to be greater than 99%.

As in our previous analyses [8, 9], the relative luminosity ratio R was obtained from crossing-by-crossing collected minimum bias (BBC) trigger counts, which measure about half of the $p+p$ inelastic cross section [21]. The uncertainty on R was derived from the comparison with a second trigger based on the Zero Degree Calorimeters [24], which selects different physics processes in a differ-

TABLE I: ΔG for different x ranges at $\mu^2 = 4 \text{ GeV}^2$ for each group's best fit and the χ^2 when comparing the expected A_{LL} in Fig. 3(a) with our data (8 degrees of freedom). Also, the minimum χ^2 and corresponding $\Delta G^{[0.02,0.3]}$ found in Fig. 3(b).

Group	Published best fit			From Fig. 3b	
	$\Delta G^{[0,1]}$	$\Delta G^{[0.02,0.3]}$	χ^2	$\Delta G^{[0.02,0.3]}$	χ^2
GS-C	0.95	0.18	8.3	0.1	8.5
DSSV	-0.05	-0.03	7.5	NA	NA
LSS	0.60	0.37	22.4	0.2	7.0
GRSV	0.67	0.38	14.8	0.2	7.1
BB	0.93	0.67	69.0	0.2	7.2

ent kinematic range. It contributed a p_T independent systematic uncertainty to A_{LL} of 7×10^{-4} .

Equation 1 is used to determine, on a fill by fill basis, A_{LL} for the yield in the π^0 mass peak for each p_T bin. The asymmetries were averaged over fills and corrected for the asymmetry in the background contribution (determined from two 50 MeV/ c^2 wide sidebands on either side of the π^0 peak) [9], which was consistent with zero.

Figure 2a shows the measured $A_{LL}^{\pi^0}$ from Run-6 [25] in comparison with our published data from the 2005 RHIC run (Run-5) [8]. The results are found to be statistically consistent with a 13% confidence level. The inset shows an expanded view of the low p_T region, as well as the relative luminosity uncertainty from Run-6. Besides this and the scale uncertainty from polarization, other systematic uncertainties that can be found by using a bunch polarization sign randomization technique and by varying the π^0 identification criteria [9] appear negligible.

Also shown in Fig. 2a are NLO pQCD predictions of $A_{LL}^{\pi^0}$ [4] based on fits of pDIS data by GRSV with three different values for ΔG at the *input* scale of $\mu^2 = 0.4$ GeV²: 1) “std”, their best fit value with $\Delta G = 0.24$, 2) $\Delta G = 0$ and 3) $\Delta G = -1.05$. The measurements are most consistent with GRSV $\Delta G = 0$. CTEQ6 unpolarized parton distribution functions (PDF) [26] were used, along with DSS fragmentation functions (FF) [27], in all calculations. Using alternative PDF [28] or FF [29] did not lead to significant differences in the A_{LL} expectations.

A_{LL} expectations based on fits to the pDIS data with a range of inputs for $\Delta G^{[0,1]}$ evolved to $\mu^2 = 0.4$ GeV² in the GRSV parameterization were calculated. Similar to our previous analysis [8], χ^2 values were calculated using our combined Run-5 and Run-6 data [25] for these expectations, effectively fitting ΔG with our data in this parameterization. In Fig. 2b, these values are plotted as a function of $\Delta G^{[0.02,0.3]}$ at $\mu^2 = 4$ GeV². Due to soft physics contamination at low p_T , we use only data with $p_T > 2$ GeV/ c [8]. Assuming that $\mu = p_T$, $\mu^2 = 4$ GeV² is then the minimum cutoff of our data. The solid curve shows the result considering only statistical uncertainties. Due to gg interactions in $p+p$ collisions, A_{LL} probes ΔG quadratically in π^0 production [4]. The χ^2 profile is thus not parabolic, and so we show $\Delta\chi^2 \equiv \chi^2 - \chi_{\min}^2 = 1$ and 9 corresponding to “1 σ ” and “3 σ ” uncertainties. The gg scattering increases toward low p_T , which dominates our statistics and causes the two minima seen in Fig. 2b. The larger allowed negative region arises from cancellation of gg and qg terms in $A_{LL}^{\pi^0}$ when ΔG is negative.

For a robust interpretation of our results in terms of ΔG , we consider not only statistical but also experimental systematic and theoretical uncertainties. The effects of the two largest experimental systematic uncertainties, due to polarization and relative luminosity, are shown in Fig. 2b. The polarization uncertainty is insignificant when extracting ΔG . However, the uncertainty on relative luminosity, though small, cannot be

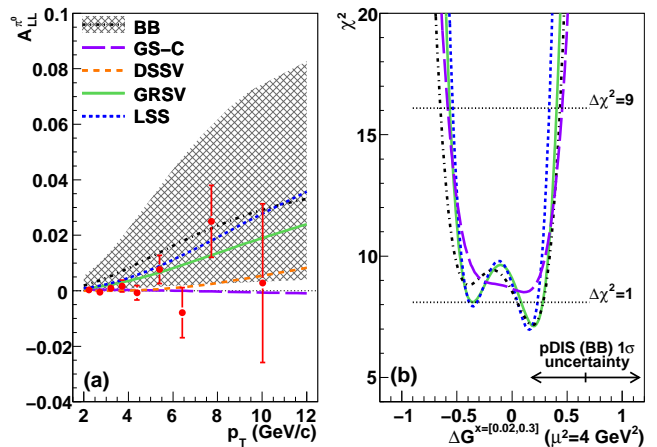


FIG. 3: (color online) (a) π^0 asymmetry expectations for different $\Delta g(x)$ in Fig. 1b. Hatched band is the pDIS uncertainty (BB). Combined Run-5 and Run-6 results are also plotted (statistical errors only). (b) The χ^2 profile as a function of $\Delta G^{[0.02,0.3]}$ for same parameterizations. Arrows indicate 1σ uncertainty on BB best fit. $\Delta\chi^2$ values are shown for GRSV.

neglected. Accounting for statistical uncertainty, we find $\Delta G_{\text{GRSV}}^{[0.02,0.3]} = 0.2 \pm 0.1$ (1σ) and $0.2^{+0.2}_{-0.8}$ (3σ) with an additional experimental systematic uncertainty of ± 0.1 .

Figure 3a shows A_{LL} expectations [4, 18] based on the parameterizations discussed above, along with the pDIS uncertainty on $\Delta g(x)$ in BB propagated to A_{LL} . Our combined Run-5 and Run-6 π^0 results [25] are also plotted for comparison. The χ^2 values for comparing each curve with our data are given in Table I. The three fit results without a node in $\Delta g(x)$ —LSS, GRSV and BB—have large values of $\Delta G^{[0.02,0.3]}$ which lead to relatively large asymmetries that lie mostly above the data, though they are consistent within the large uncertainty from pDIS. For GS-C and DSSV, which have a node in $\Delta g(x)$ near the center of the sampled x region, a cancellation between the positive and negative contribution in the wide x distribution in each p_T bin leads to a small value of $\Delta G^{[0.02,0.3]}$ and thus small A_{LL} . As these two parameterizations have significantly different $\Delta G^{[0,1]}$ values, it is clear that we are sensitive only to $\Delta G^{[0.02,0.3]}$.

For each pDIS fit, by varying $\Delta G^{[0,1]}$ at the input scale while fixing the quark distributions and the shape of $\Delta g(x)$ to the best fit values, a range of A_{LL} curves were generated. Figure 3b shows the resulting χ^2 profiles. While this approach is different from that in Fig. 2b, resulting in a different χ^2 profile shape for GRSV, the $\Delta\chi^2=1$ and 9 constraints are quite consistent. The $\Delta G^{[0.02,0.3]}$ values at the χ^2 minimum for each parameterization are between 0.1 and 0.2, and are listed in Table I. At $\Delta\chi^2=9$, the profiles are consistent for all parameterizations, independent of shape, indicating that our data are primarily sensitive to the size of $\Delta G^{[0.02,0.3]}$.

The cross section for π^0 production has been pre-

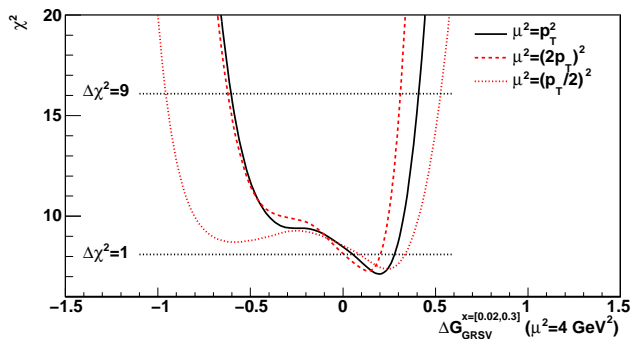


FIG. 4: (color online) χ^2 profile as a function of $\Delta G_{\text{GRSV}}^{[0.02,0.3]}$ when the theoretical scale is set to $\mu = p_T$, $p_T/2$ and $2p_T$.

sented [8] and compared with NLO pQCD expectations with the theoretical scales (factorization, fragmentation, and renormalization) in the calculation all set equal to $\mu = kp_T$ with $k = 1$. The calculation agreed with our results within the sizable theoretical uncertainties in the choice of scale, which were estimated by varying k up and down by a factor of two. As we rely on NLO pQCD to extract $\Delta G_{\text{GRSV}}^{[0.02,0.3]}$ from our measured $A_{\text{LL}}^{\pi^0}$, we must consider the effect of this uncertainty. Figure 4 shows the change in the $\Delta G_{\text{GRSV}}^{[0.02,0.3]}$ constraint when varying k in the A_{LL} calculation in the GRSV parameterization. The theoretical scale uncertainty for the constraint on positive values of $\Delta G_{\text{GRSV}}^{[0.02,0.3]}$ is similar to that for varying the parameterization, while large uncertainty arises for negative values.

We have presented results for $A_{\text{LL}}^{\pi^0}$ from Run-6, which, combined with Run-5 results, at $\mu^2 = 4 \text{ GeV}^2$ give

$$\Delta G_{\text{GRSV}}^{[0.02,0.3]} = 0.2 \pm 0.1(\text{stat}) \pm 0.1(\text{sys}) \\ \pm_{-0.4}^{+0.0}(\text{shape}) \pm 0.1(\text{scale}). \quad (2)$$

Using four parameterizations of $\Delta g(x)$, we find a shape independent constraint of $-0.7 < \Delta G_{\text{GRSV}}^{[0.02,0.3]} < 0.5$ at $\Delta\chi^2=9$ ($\sim 3\sigma$). The theoretical scale induced uncertainty is small for positive values of $\Delta G_{\text{GRSV}}^{[0.02,0.3]}$, but is sizable for negative values. Future measurements will be required to measure $\Delta g(x)$ for $x < 0.02$ where large uncertainty remains [11] and which may still contribute a significant amount of the proton spin. The quark spin contribution was well constrained by pDIS, and our result begins to significantly constrain the gluon spin contribution as well.

We thank the staff of the Collider-Accelerator and Physics Departments at BNL for their vital contributions. We acknowledge support from the Office of Nuclear Physics in DOE Office of Science, NSF, and a

sponsored research grant from Renaissance Technologies (U.S.), MEXT and JSPS (Japan), CNPq and FAPESP (Brazil), NSFC (China), MSMT (Czech Republic), IN2P3/CNRS, and CEA (France), BMBF, DAAD, and AvH (Germany), OTKA (Hungary), DAE (India), ISF (Israel), KRF and KOSEF (Korea), MES, RAS, and FAAE (Russia), VR and KAW (Sweden), U.S. CRDF for the FSU, US-Hungary Fulbright, US-Israel BSF.

* Deceased

† PHENIX Spokesperson: jacak@skipper.physics.sunysb.edu

- [1] J. Ashman et al., Nucl. Phys. **B328**, 1 (1989).
- [2] A. Airapetian et al., Phys. Rev. D **75**, 012007 (2007).
- [3] V. Y. Alexakhin et al., Phys. Lett. **B647**, 8 (2007).
- [4] B. Jäger, A. Schäfer, M. Stratmann, and W. Vogelsang, Phys. Rev. D **67**, 054005 (2003).
- [5] J. Adams et al., Phys. Rev. Lett. **92**, 171801 (2004).
- [6] B. I. Abelev et al., Phys. Rev. Lett. **97**, 252001 (2006).
- [7] S. S. Adler et al., Phys. Rev. D **71**, 071102 (2005).
- [8] A. Adare et al., Phys. Rev. D **76**, 051106 (2007).
- [9] S. S. Adler et al., Phys. Rev. Lett. **93**, 202002 (2004).
- [10] S. S. Adler et al., Phys. Rev. D **73**, 091102 (2006).
- [11] D. de Florian, R. Sassot, M. Stratmann, and W. Vogelsang, Phys. Rev. Lett. **101**, 072001 (2008).
- [12] M. Glück, E. Reya, M. Stratmann, and W. Vogelsang, Phys. Rev. D **63**, 094005 (2001).
- [13] J. Bluemlein and H. Bottcher, Nucl. Phys. **B636**, 225 (2002).
- [14] E. Leader, A. V. Sidorov, and D. B. Stamenov, Phys. Rev. D **73**, 034023 (2006).
- [15] T. Gehrmann and W. J. Stirling, Phys. Rev. D **53**, 6100 (1996).
- [16] B. I. Abelev et al., Phys. Rev. Lett. **100**, 232003 (2008).
- [17] M. Sarsour, *2007 APS DNP meeting, Newport News, Virginia, Oct. 2007*.
- [18] M. Stratmann (2007), private communication.
- [19] S. S. Adler et al., Phys. Rev. D **74**, 072002 (2006).
- [20] L. Aphecetche et al., Nucl. Instrum. Meth. **A499**, 521 (2003).
- [21] S. S. Adler et al., Phys. Rev. Lett. **91**, 241803 (2003).
- [22] M. Allen et al., Nucl. Instrum. Meth. **A499**, 549 (2003).
- [23] Y. Fukao et al., Phys. Lett. **B650**, 325 (2007).
- [24] M. Allen et al., Nucl. Instrum. Meth. **A470**, 488 (2001).
- [25] Tables of data available at http://www.phenix.bnl.gov/WWW/info/data/ppg091_data.html.
- [26] J. Pumplin et al., JHEP **07**, 012 (2002).
- [27] D. de Florian, R. Sassot, and M. Stratmann, Phys. Rev. D **75**, 114010 (2007).
- [28] A. D. Martin, R. G. Roberts, W. J. Stirling, and R. S. Thorne, Eur. Phys. J. **C28**, 455 (2003).
- [29] B. A. Kniehl, G. Kramer, and B. Potter, Nucl. Phys. **B582**, 514 (2000).